Almost exact energies for the Gaussian-2 set with the semistochastic heat-bath configuration interaction method

Yuan Yao, ^{1, a)} Emmanuel Giner, ^{2, b)} Junhao Li, ^{1, c)} Julien Toulouse, ^{2, 3, d)} and C. J. Umrigar^{1, e)}
¹⁾ Laboratory of Atomic and Solid State Physics, Cornell University, Ithaca, New York 14853,
United States

(Dated: 11 October 2024)

The recently developed semistochastic heat-bath configuration interaction (SHCI) method is a systematically improvable selected configuration interaction plus perturbation theory method capable of giving essentially exact energies for larger systems than is possible with other such methods. We compute SHCI atomization energies for 55 molecules which have been used as a test set in prior studies because their atomization energies are known from experiment. Basis sets from cc-pVDZ to cc-pV5Z are used, totaling up to 500 orbitals and a Hilbert space of 10^{32} Slater determinants for the largest molecules. For each basis, an extrapolated energy within chemical accuracy (1 kcal/mol or 1.6 mHa/mol) of the exact energy for that basis is computed using only a tiny fraction of the entire Hilbert space. We also use our almost exact energies to benchmark coupled-cluster [CCSD(T)] energies. The energies are extrapolated to the complete basis set limit and compared to the experimental atomization energies. The extrapolations are done both without and with a basis-set correction based on density-functional theory. The mean absolute deviations from experiment for these extrapolations are 0.71 kcal/mol and 0.61 kcal/mol, respectively. Orbital optimization methods used to obtain improved convergence of the SHCI energies are also discussed.

I. INTRODUCTION

The recently developed semistochastic heat-bath configuration interaction (SHCI) method $^{1-7}$ is a systematically improvable quantum chemistry method capable of providing essentially exact energies for small manyelectron systems. It has been successfully applied to a number of challenging problems in quantum chemistry, including the potential energy curve of the chromium dimer⁸ for which coupled cluster with single, double, and perturbative triple excitations [CCSD(T)], the gold standard of single-reference quantum chemistry, does not give even a qualitatively correct description. It has also been used as the reference method for calculations on transition metal atoms, ions, and monoxides 9 to test the accuracy of a wide variety of other electronic-structure methods.

SHCI is an example of the selected configuration interaction (SCI) plus perturbation theory (SCI+PT) methods¹⁰⁻²¹ which have two stages. In the first stage a variational wave function is constructed iteratively, starting from a determinant that is expected to have a significant amplitude in the final wave function, e.g., the Hartree-Fock (HF) determinant. The number of determinants in the variational wave function is controlled by a parameter ϵ_1 . In the second stage, second-order perturbation theory is used to improve upon the variational energy.

In this paper, the SHCI method is reviewed in Section II, our orbital optimization schemes are described in Section III, the basis-set correction and extrapolation that we use are indicated in Section IV, and the details of the calculations are given in Section V. In Section VI we apply SHCI to the 55 first- and second-row molecules that served as the training set for the Gaussian-2 (G2) protocol²² because accurate experimental atomization energies were believed to be known for them. The G2 protocol is one of several quantum chemistry composite methods that combine low-order methods on large basis sets and high-order coupled-cluster methods on smaller basis sets to compute accurate thermochemical properties (see, e.g., Refs. 23–27.). These 55 molecules, which we refer to as the G2 set, have previously been used to test the accuracy of coupled-cluster-based methods²⁴ and quantum Monte Carlo (QMC) methods^{28–31}. We employ the correlation consistent basis sets cc-pVnZ for n = 2 (D), 3 (T), 4 (Q), and 5, keeping the core electrons frozen, to obtain SHCI energies that we believe are well within 1 mHa of the exact energies for each of the molecules and basis sets. Hence these calculations provide a set of reference energies that can be used to test other accurate electronic-structure methods.

The molecules in the G2 set are sufficiently weakly correlated that one would expect CCSD(T) to be rea-

²⁾Laboratoire de Chimie Théorique, Sorbonne Université and CNRS, F-75005 Paris, France

³⁾Institut Universitaire de France, F-75005 Paris, France

The total energy (sum of the variational energy and the perturbative correction) is computed at several values of ϵ_1 and extrapolated to $\epsilon_1 \to 0$ to obtain an estimate for the full configuration interaction (FCI) energy. The efficiency of SHCI depends on the choice of the orbitals – natural orbitals lead to faster convergence of the energy relative to HF orbitals and optimized orbitals yield yet faster convergence.

a) Electronic mail: yy682@cornell.edu

b) Electronic mail: emmanuel.giner@lct.jussieu.fr

c) Electronic mail: jl2922@cornell.edu

d) Electronic mail: toulouse@lct.jussieu.fr

e) Electronic mail: cyrusumrigar@cornell.edu

sonably accurate, but not at the level of 1 mHa. Hence, we calculate also the CCSD(T) energies using the same basis sets in order to use SHCI to evaluate the errors in the CCSD(T) energies, as FCI is not feasible for most of these systems. The SHCI energies are then extrapolated to the complete-basis-set (CBS) limit, both without and with a basis-set correction based on density-functional theory (DFT)^{32–35}. Corrections taken from the literature for zero-point energy, relativistic effects, and corevalence correlation are then applied to obtain our predictions for the atomization energies, which are then compared to the best available experimental values. For some systems the available experimental values differ substantially from each other and for at least one system we believe that the theoretical estimates are more accurate than the best experimental value.

II. REVIEW OF THE SHCI METHOD

In this section, we review the SHCI method, emphasizing the two important ways it differs from other SCI+PT methods. In the following, we use $\mathcal V$ for the set of variational determinants, and $\mathcal P$ for the set of perturbative determinants, that is, the set of determinants that are connected to the variational determinants by at least one non-zero Hamiltonian matrix element but are not present in $\mathcal V$.

A. Variational stage

SHCI starts from an initial determinant and generates the variational wave function through an iterative process. At each iteration, the variational wave function, Ψ_V , is written as a linear combination of the determinants in the space $\mathcal V$

$$|\Psi_V\rangle = \sum_{D_i \in \mathcal{V}} c_i |D_i\rangle$$
 (1)

and new determinants, D_a , from the space \mathcal{P} that satisfy the criterion

$$\exists D_i \in \mathcal{V}, \text{ such that } |H_{ai}c_i| > \epsilon_1$$
 (2)

are added to the \mathcal{V} space, where H_{ai} is the Hamiltonian matrix element between determinants D_a and D_i , and ϵ_1 is a user-defined parameter that controls the accuracy of the variational stage³⁶. (When $\epsilon_1 = 0$, the method becomes equivalent to FCI.) After adding the new determinants to \mathcal{V} , the Hamiltonian matrix is constructed, and diagonalized using the diagonally preconditioned Davidson method³⁷, to obtain an improved estimate of the lowest eigenvalue, E_V , and eigenvector, Ψ_V . This process is repeated until the change in the variational energy E_V falls below a certain threshold.

Other SCI methods use different criteria, based on either the first-order perturbative coefficient of the wave

function,

$$\left| c_a^{(1)} \right| = \left| \frac{\sum_i H_{ai} c_i}{E_V - E_a} \right| > \epsilon_1 \tag{3}$$

or the second-order perturbative correction to the energy,

$$-\Delta E^{(2)} = -\frac{(\sum_{i} H_{ai} c_{i})^{2}}{E_{V} - E_{a}} > \epsilon_{1}, \tag{4}$$

where $E_a = H_{aa}$. The reason we choose instead the selection criterion in Eq. (2) is that it can be implemented very efficiently without checking the vast majority of the determinants that do not meet the criterion, by taking advantage of the fact that most of the Hamiltonian matrix elements correspond to double excitations, and their values do not depend on the determinants themselves but only on the four orbitals whose occupancies change during the double excitation. Therefore, at the beginning of an SHCI calculation, for each pair of spin-orbitals, the absolute values of the Hamiltonian matrix elements obtained by doubly exciting from that pair of orbitals is computed and stored in decreasing order by magnitude, along with the corresponding pairs of orbitals the electrons would excite to. Then the double excitations that meet the criterion in Eq. (2) can be generated by looping over all pairs of occupied orbitals in the reference determinant, and traversing the array of sorted doubleexcitation matrix elements for each pair. As soon as the cutoff is reached, the loop for that pair of occupied orbitals is exited. Although the criterion in Eq. (2) does not include information from the diagonal elements, this selection criterion is not significantly different from either of the criteria in Eqs. (3) and (4) because the terms in the numerators of Eqs. (3) and (4) span many orders of magnitude, so the sums are highly correlated with the largest-magnitude term in the sums in Eq. (3) or Eq. (4), and because the denominator is never small after several determinants have been in V. It was demonstrated in Ref. 1 that the selected determinants give only slightly inferior convergence to those selected using the criterion in Eq. (3). This is greatly outweighed by the improved selection speed. Moreover, one could use the criterion in Eq. (2) with a smaller value of ϵ_1 as a preselection criterion, and then select determinants using the criterion in Eq. (4) or something close to it, thereby having the benefit of both a fast selection method and a close to optimal choice of determinants. We use a similar, but somewhat more complicated criterion, also for the selection of the determinants connected to those in V by a single excitation, but this improvement is of lesser importance because the number of such determinants is much smaller. With these improvements the time required for selecting determinants is negligible, and the most time consuming step by far in the variational stage is the construction of the sparse Hamiltonian matrix. Details for doing this efficiently are given in Ref. 7.

B. Perturbative stage

In common with most other SCI+PT methods, the perturbative correction is computed using Epstein-Nesbet perturbation theory 38,39 . The variational wave function is used to define the zeroth-order Hamiltonian, $\hat{H}^{(0)}$, and the perturbation, $\hat{H}^{(1)}$,

$$\hat{H}^{(0)} = \sum_{D_i, D_j \in \mathcal{V}} H_{ij} |D_i\rangle \langle D_j| + \sum_{D_a \notin \mathcal{V}} H_{aa} |D_a\rangle \langle D_a|.$$

$$\hat{H}^{(1)} = \hat{H} - \hat{H}^{(0)}.$$
(5)

The first-order energy correction is zero, and the secondorder energy correction $\Delta E^{(2)}$ is

$$\Delta E^{(2)} = \langle \Psi_V | \hat{H}^{(1)} | \Psi^{(1)} \rangle = \sum_{D_a \in \mathcal{P}} \frac{\left(\sum_{D_i \in \mathcal{V}} H_{ai} c_i \right)^2}{E_V - E_a} (6)$$

where $\Psi^{(1)}$ is the first-order wave-function correction.

It is expensive to evaluate the expression in Eq. (6) because the outer summation includes all determinants in the space \mathcal{P} and their number is $\mathcal{O}(N_e^2 N_v^2 N_v)$, where $N_{\mathcal{V}}$ is the number of variational determinants, $N_{\rm e}$ is the number of electrons, and $N_{\rm v}$ is the number of unoccupied orbitals. The straightforward and time-efficient approach to computing the perturbative correction requires storing the partial sum $\sum_{i \in \mathcal{V}} H_{ai} c_i$ for each unique a, while looping over all the determinants $i \in \mathcal{V}$. This creates a severe memory bottleneck. An alternative approach, which is widely used, does not require storing the unique a, but requires checking whether the determinant was already generated by checking its connection with variational determinants whose connections have already been included. This entails some additional computational expense.

The SHCI algorithm instead uses two other strategies to reduce both the computational time and the storage requirement. First, SHCI screens the sum¹ using a second threshold, ϵ_2 (where $\epsilon_2 < \epsilon_1$) as the criterion for selecting perturbative determinants \mathcal{P} ,

$$\Delta E^{(2)}(\epsilon_2) = \sum_{a} \frac{\left(\sum_{D_i \in \mathcal{V}}^{(\epsilon_2)} H_{ai} c_i\right)^2}{E_V - E_a} \tag{7}$$

where $\sum_{i=0}^{(\epsilon_2)}$ indicates that only terms in the sum for which $|H_{ai}c_i| \geq \epsilon_2$ are included. Similar to the variational stage, we find the connected determinants efficiently with precomputed arrays of double excitations sorted by the magnitude of their Hamiltonian matrix elements¹. Note that the vast number of terms that do not meet this criterion are never evaluated.

Even with this screening, the simultaneous storage of all terms indexed by a in Eq. (7) can exceed computer memory when ϵ_2 is chosen small enough to obtain essentially the exact perturbation energy. The second innovation in the calculation of the SHCI perturbative correction is to overcome this memory bottleneck by evaluating it semistochastically. The most important contributions

are evaluated deterministically and the rest are sampled stochastically. Our original method used a two-step perturbative algorithm², but our later three-step perturbative algorithm⁷ is even more efficient. The three steps are:

- 1. A deterministic step with cutoff $\epsilon_2^{\text{dtm}}(<\epsilon_1)$, wherein all the variational determinants are used, and all the perturbative batches are summed over.
- 2. A "pseudo-stochastic" step, with cutoff $\epsilon_2^{\text{psto}}(<\epsilon_2^{\text{dtm}})$, wherein all the variational determinants are used, but the perturbative determinants are partitioned into batches. Typically only a small fraction of these batches need be summed over to achieve an error much smaller than the target error.
- 3. A stochastic step, with cutoff $\epsilon_2(<\epsilon_2^{\text{psto}})$, wherein a few stochastic samples of variational determinants, each consisting of N_d determinants, are sampled with probability $c_i/\sum_{i\in\mathcal{V}}c_i$, and only one of the perturbative batches is randomly selected per variational sample.

We note that, subsequent to our first semistochastic paper², a completely different, but also efficient, semistochastic approach has been presented in Ref. 18.

III. ORBITAL OPTIMIZATION

SHCI gives an estimate of the exact FCI energy by extrapolating energies evaluated at several $\epsilon_1 > 0$ to $\epsilon_1 = 0$, the FCI limit. This results in an extrapolation error that disappears in the limit that the extrapolation distance (difference in energy at the smallest value of ϵ_1 used and at $\epsilon_1 = 0$) goes to zero.

The extrapolation distance can be reduced by decreasing ϵ_1 , but this is limited by the available computer memory and time. An alternative approach is to optimize the orbitals to obtain more compact configuration-interaction (CI) expansions with lower variational energies.

The first step to orbital optimization is to find the SHCI natural orbitals, i.e., the eigenstates of the one-body reduced density matrix. These orbitals have a definite occupation number for a given variational wave function and the most occupied ones in some sense represent the most important degrees of freedom.

Orbitals can be further optimized by directly minimizing the energy of the variational wave function through the orbital rotation parameters X:

$$E(\mathbf{X}) = \langle \Psi_V | \exp(\hat{X}) \hat{H} \exp(-\hat{X}) | \Psi_V \rangle, \tag{8}$$

where \hat{X} is a real antihermitian operator such that $\exp(-\hat{X})$ parameterizes orthogonal transformations in orbital space. For a system with $N_{\rm orb}$ orbitals, this yields at most $N_{\rm orb}(N_{\rm orb}-1)/2$ orbital optimization parameters, which are the elements of the real antisymmetric matrix \mathbf{X} . In reality, the number of parameters will often

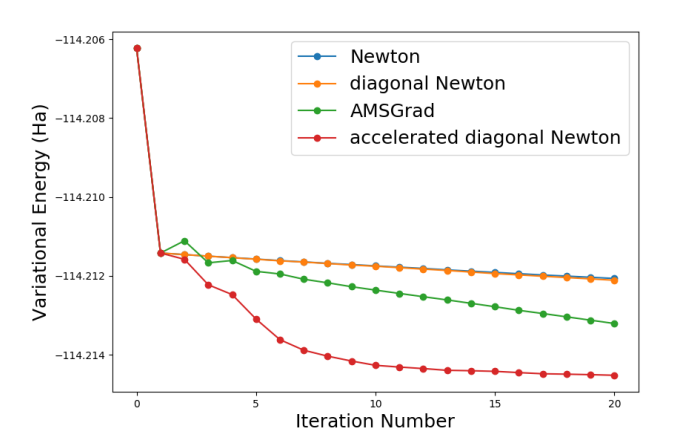


FIG. 1. Comparison of four orbital optimization schemes for the $\rm H_2CO$ molecule in the cc-pVDZ basis and threshold parameter $\epsilon_1 = 2 \times 10^{-4}$. All four calculations start with HF orbitals and construct natural orbitals on the first iteration, so they differ only from the second iteration on. The Newton and diagonal Newton curves are nearly coincident for this system.

be less than this due to point group symmetry. Depending on the particular optimization algorithm used, the gradient and sometimes part of the Hessian of the energy with respect to the orbital parameters are needed, either of which requires computing both the one- and two-body density matrices of the variational wave function. In addition to the orbital parameters, the CI parameters (which are much more numerous) must be optimized as well.

A. Newton's method

The Newton method is a straightforward method for optimizing the parameters. The parameters \mathbf{x}_{t+1} at iteration t+1 are given by

$$\mathbf{x}_{t+1} = \mathbf{x}_t - \mathbf{h}_t^{-1} \mathbf{g}_t. \tag{9}$$

where \mathbf{g}_t and \mathbf{h}_t are the gradient and the Hessian of the energy with respect to the parameters at iteration t. In practice it is more efficient to find the parameter changes by solving the set of linear equations:

$$\mathbf{h}_t \left(\mathbf{x}_{t+1} - \mathbf{x}_t \right) = -\mathbf{g}_t. \tag{10}$$

However, the problem is that the number of parameters is typically much too large for even this to be practical. Typically, even using a rather large value of the threshold parameter ϵ_1 for the optimization step, there are millions of CI parameters whereas there are only thousands of orbital parameters. So, one resorts to alternating the optimization of the CI parameters using the usual Davidson algorithm, and optimizing the orbital parameters in the much smaller space of orbital rotations using the Newton method. This alternating optimization often converges

very slowly because the coupling between the CI parameters and the orbital parameters is strong as can be seen in Fig. 1. Note that the orbital optimization problem in SHCI is more difficult than that in the usual complete-active-space self-consistent-field (CASSCF) method for two reasons. First, none of the orbital rotations among orbitals of the same symmetry are redundant, so the number of orbital parameters that need to be optimized is much larger. Second, the coupling between the CI parameters and the orbital parameters is stronger.

In quantum chemistry problems, the orbital part of the Hessian matrix is often diagonally dominant. In that case one can save significant computer time by ignoring the off-diagonal elements. We refer to this as the "diagonal Newton" method, and Fig. 1 shows that for this molecule it converges at the same rate as the Newton method. The convergence of both methods is limited by the lack of coupling between the CI and orbital parameters.

B. AMSGrad

AMSGrad is a momentum-based gradient-descent method commonly used in machine learning⁴⁰. It avoids the expensive Hessian calculations since only gradient information is needed. At each iteration, it employs running averages of the gradient components and their squares, determined by the mixing parameters $\beta_1, \beta_2 \in (0,1)$, according to

$$\mathbf{m}_{t} = \beta_{1} \mathbf{m}_{t-1} + (1 - \beta_{1}) \mathbf{g}_{t},$$

$$v_{t} = \beta_{2} v_{t-1} + (1 - \beta_{2}) \mathbf{g}_{t}^{2},$$

$$\hat{v}_{t} = \max(\hat{v}_{t-1}, v_{t}),$$

$$\mathbf{x}_{t+1} = \mathbf{x}_{t} - \frac{\eta}{\sqrt{\hat{v}_{t}} + \epsilon} \mathbf{m}_{t}.$$
(11)

The learning parameters η, β_1 , and β_2 together determine the level of aggressiveness of the descent and ϵ is a small constant for numerical stability. We have found empirically that with a suitable level of aggressiveness, AMSGrad oscillates for the first few iterations but eventually descends at a much quicker pace per iteration compared to either Newton or diagonal Newton, as can be seen in Fig. 1. In addition each iteration takes less time since only the gradient is needed. For a variety of systems we have found that the parameters $\eta = 0.01, \beta_1 = 0.5, \beta_2 = 0.5$ give reasonably good convergence, even though they are much different from the values recommended in the literature.

C. Accelerated Newton's method

Finally, we have developed a heuristic overshooting method that achieves yet better convergence for most systems. Here, the overshooting tries to account for the coupling between CI and orbital parameters, but it may be more generally useful whenever alternating optimization of subsets of parameters is done.

At each iteration, a diagonal Newton step is calculated for the orbital parameters, but, instead of using the proposed step, it is amplified by a factor f_t determined by the cosine of the angle between the previous step $\mathbf{x}_t - \mathbf{x}_{t-1}$ and the current step $\mathbf{x}_{t+1} - \mathbf{x}_t$:

$$f_t = \min\left(\frac{1}{2 - \cos(\mathbf{x}_t - \mathbf{x}_{t-1}, \mathbf{x}_{t+1} - \mathbf{x}_t)}, \frac{1}{\epsilon}\right)$$
(12)

where ϵ is initialized to 0.01 and $\epsilon \leftarrow \epsilon^{0.8}$ each time $\cos(\mathbf{x}_t - \mathbf{x}_{t-1}, \mathbf{x}_{t+1} - \mathbf{x}_t) < 0$. The cosine in the expression is calculated in a "scale-invariant" way to make it invariant under a rescaling of some of the parameters, i.e., in the usual definition $\cos(\mathbf{v}, \mathbf{w}) = \langle \mathbf{v}, \mathbf{w} \rangle / \sqrt{\langle \mathbf{v}, \mathbf{v} \rangle \langle \mathbf{w}, \mathbf{w} \rangle}$ we define the inner product as $\langle \mathbf{v}, \mathbf{w} \rangle = \mathbf{v}^T \mathbf{h} \mathbf{w}$, where the Hessian h can again be approximated by its diagonal. Another scale invariant choice for the inner product is $\langle \mathbf{v}, \mathbf{w} \rangle = \mathbf{v}^T \mathbf{g} \mathbf{g}^T \mathbf{w}$, and that works equally well.

As shown in Fig. 1, this accelerated scheme optimizes much faster than the previous schemes. For instance, after 4 iterations, the gain in variational energy is already better than that after 20 iterations using the conventional Newton method with the diagonal approximation. Compared to AMSGrad, the higher per iteration cost is more than made up by the greatly reduced number of iterations needed. For this system, not only does the energy drop significantly but the number of determinants decreases as well. For the accelerated scheme the drop is from 145,370 to 93,882 determinants. However, for some systems the number of determinants increases, thereby partly offsetting the benefit of the energy gain.

BASIS-SET CORRECTION AND EXTRAPOLATION

We employ the correlation consistent polarized valence (cc-pVnZ) basis sets with n = 2 (D), 3 (T), 4 (Q), 5. The energies computed for each atom or molecule are extrapolated to the CBS limit using separate extrapolations for the HF energy and the correlation energy, 41-43

$$E_{\text{CBS}}^{\text{HF}} = E_n^{\text{HF}} + a \exp\left(-bn\right), \tag{13}$$

$$E_{\text{CBS}}^{\text{corr}} = E_n^{\text{corr}} + cn^{-3}, \tag{14}$$

$$E_{\text{CBS}}^{\text{corr}} = E_n^{\text{corr}} + cn^{-3},\tag{14}$$

where n is the cardinal number of the basis set. For the HF part, basis sets with n = 3 (T), 4 (Q), 5 are used, and for the correlation part, only n = 4 (Q), 5 are used. The only exceptions are the one-electron systems, H, Li, and Na, for which the lowest HF energy is taken as the CBS energy.

To estimate the total energies in the CBS limit, we also employ the DFT-based basis-set correction recently developed in Refs. 32–35. In this scheme, the total SHCI energy in a given basis set is corrected as

$$E_n^{\rm SHCI+PBE} = E_n^{\rm SHCI} + \bar{E}_n^{\rm PBE}[\rho, \zeta, \mu], \qquad (15)$$

where $\bar{E}_{n}^{\mathrm{PBE}}[\rho,\zeta,\mu]$ is a basis-set-dependent functional of the density $\rho(\mathbf{r})$, the spin polarization $\zeta(\mathbf{r}) = [\rho_{\uparrow}(\mathbf{r}) \rho_{\perp}(\mathbf{r}) / \rho(\mathbf{r})$, and the local range-separation function $\mu(\mathbf{r})$

$$\bar{E}_n^{\mathrm{PBE}}[\rho,\zeta,\mu] = \int \rho(\mathbf{r}) \bar{\varepsilon}_{\mathrm{c,md}}^{\mathrm{sr,PBE}}(\rho(\mathbf{r}),\zeta(\mathbf{r}),\mu(\mathbf{r})) \mathrm{d}\mathbf{r}.(16)$$

In Eq. (16), $\bar{\varepsilon}_{\rm c,md}^{\rm sr,PBE}$ is the complementary short-range correlation energy per particle with multideterminant reference (md) that was constructed in Ref. 33 based on the Perdew-Burke-Ernzerhof (PBE)⁴⁴ correlation functional and the on-top pair density of the uniform-electron gas. The local range-separation function $\mu(\mathbf{r})$ provides a local measure of the incompleteness of the basis set and is defined as

$$\mu(\mathbf{r}) = \frac{\sqrt{\pi}}{2} W(\mathbf{r}, \mathbf{r}), \tag{17}$$

where $W(\mathbf{r}, \mathbf{r})$ is the on-top value of the effective twoelectron interaction in the basis set

$$W(\mathbf{r}, \mathbf{r}) = \begin{cases} f(\mathbf{r}, \mathbf{r}) / n_2(\mathbf{r}, \mathbf{r}), & \text{if } n_2(\mathbf{r}, \mathbf{r}) \neq 0, \\ \infty, & \text{otherwise,} \end{cases}$$
(18)

$$f(\mathbf{r}, \mathbf{r}) = \sum_{pq \in \mathcal{B}} \sum_{rstu \in \mathcal{A}} \phi_p(\mathbf{r}) \phi_q(\mathbf{r}) V_{pq}^{rs} \Gamma_{rs}^{tu} \phi_t(\mathbf{r}) \phi_u(\mathbf{r}), \quad (19)$$

$$n_2(\mathbf{r}, \mathbf{r}) = \sum_{rstu \in A} \phi_r(\mathbf{r}) \phi_s(\mathbf{r}) \Gamma_{rs}^{tu} \phi_t(\mathbf{r}) \phi_u(\mathbf{r}), \qquad (20)$$

where $V_{pq}^{rs} = \langle pq|rs \rangle$ are the two-electron integrals and Γ_{rs}^{tu} is the opposite-spin two-body density matrix. Since $\mu(\mathbf{r})$ is very weakly dependent on Γ_{rs}^{tu} , we calculate Γ_{rs}^{tu} at the HF level only. Consistently, $\{\phi_p(\mathbf{r})\}$ are the HF orbitals, and $\rho(\mathbf{r})$ and $\zeta(\mathbf{r})$ are also calculated at the HF level. Since the core electrons are frozen in SHCI, we use the frozen-core variant^{33,35} of this DFT basis-set correction which means that in Eqs. (19) and (20) the sums over r, s, t, u are restricted to the set of active (i.e., non-core) occupied HF orbitals A. Yet, the local range-separation function $\mu(\mathbf{r})$ probes the entire basis set through the sums over p, q which run over the set of all (occupied + virtual) HF orbitals \mathcal{B} .

For a fixed basis set, the energy functional $\bar{E}_n^{\mathrm{PBE}}[
ho,\zeta,\mu]$ provides an estimate of the energy missing in FCI to reach the CBS limit. It has the desirable property of vanishing in the CBS limit, i.e. $\bar{E}_{\text{CBS}}^{\text{PBE}} = 0$, and thus the DFT basis-set correction does not alter the CBS limit, i.e. $E_{\rm CBS}^{\rm SHCI+PBE}=E_{\rm CBS}^{\rm SHCI}$, but just accelerates the basis convergence.

Based on the analysis of basis convergence in rangeseparated DFT⁴⁵, we assume an exponential basis convergence of $E_n^{\rm SHCI+PBE}$ which gives us another estimate of the CBS limit of $E_n^{\rm SHCI}$ via the extrapolation

$$E_{\mathrm{CBS}}^{\mathrm{SHCI+PBE}} = E_n^{\mathrm{SHCI+PBE}} + a \exp{(-bn)}, \quad (21)$$

using n = 3 (T), 4 (Q), 5. The only exceptions are Be and Cl, whose cc-pV5Z energy is higher than the cc-pVQZ energy and for which the cc-pV5Z energy is taken as the CBS energy.

V. COMPUTATIONAL DETAILS

The HF and CCSD(T) calculations are done with PySCF⁴⁶ or MOLPRO⁴⁷. The starting integrals are computed for HF orbitals. The core orbitals are kept fixed

for all the subsequent steps. Then we construct integrals in the SHCI natural orbital basis by computing and diagonalizing the one-body density matrix and rotating the integrals in the HF basis to the natural orbital basis. Next we use the methods discussed in Section III to construct the integrals in the optimized orbital basis. We use a fairly large value of ϵ_1 (typically 2×10^{-4}) to construct the natural orbitals and the optimized orbitals. For some systems the natural orbital basis is reasonably close to the optimal one, but for most systems the optimized orbital bases result in considerable gains in efficiency. The final SHCI calculations using the optimized orbitals employ a smaller value of ϵ_1 (typically below 4×10^{-5}).

The PBE-based basis-set correction described in Section IV is calculated independently from the SHCI calculations using the software QUANTUM PACKAGE⁴⁸. If the HF two-body density matrix is used in Eqs. (19) and (20), the basis-set correction has a computational cost of $\mathcal{O}(N_{\rm g}N_{\rm e}^2N_{\rm orb}^2)$ where $N_{\rm g}$ is the number of realspace grid points used for numerical integration in Eq. (16) and here $N_{\rm orb}$ is the total number of orbitals (including core orbitals) in the basis set. The two-electron integrals in the HF orbital basis, involving up to two virtual orbitals, are also needed and the cost for doing the integral transformation to compute these is $\mathcal{O}(N_{\rm e}^2 N_{\rm orb}^3)$. However, most of these integrals (aside from those involving the core orbitals) are needed for SHCI anyway. So, the DFT-based basis-set correction does not increase the computational time of SHCI calculations appreciably.

The geometries are taken from the Supplementary Material of Ref. 30, which in turn took them from the papers cited therein. They are provided in the Supplemental Materials⁴⁹. In order to compare to experimental atomization energies, the CBS SHCI energies are corrected for zero-point energies (ZPE), core-valence correlation (CV), scalar relativity (SR), and spin-orbit (SO) effects. We take the corrections from the literature. Since most of the papers do not have all the 55 molecules we studied, we take the corrections from Refs. 24 and 50 in that order, i.e., we take it from the first of these references that contains corrections for that molecule. The source of the corrections is indicated in Table I next to the entry for core-valence correction (CV). Similarly the experimental values quoted in Table I are taken from Refs. 24, 51-53 in that order.

VI. RESULTS

We have computed the total energies for each of the 55 molecules and their 12 constituent atoms in the four basis sets mentioned in Section IV. The accuracy of these energies should be considerably better than 1 mHa, as discussed later in this section. These energies are provided in CSV files in the Supplementary Materials⁴⁹ and can serve as a reference for other approximate methods. In particular, we have used it to test the accuracy of CCSD(T). None of the 67 systems studied is strongly correlated, so one would expect the CCSD(T) energies

to be reasonably accurate. This is in fact the case as can be seen from Fig. 2 which shows the deviation of the CCSD(T) total energies from the SHCI total energies. CCSD(T) deviates from SHCI by 1-2 mHa for the lighter systems and 3-4 mHa for the heavier ones. For systems with two or fewer valence electrons, the two methods agree exactly as they must, and for all the systems with more electrons, CCSD(T) underestimates the correlation energy. The mean absolute deviation (MAD) is roughly independent of the basis size, being 1.00, 1.07, 1.10, and 1.06 mHa, respectively, for the four basis sets. The pattern of the errors is very similar for the four basis sets. Although the absolute value of the correlation energy grows with the size of the basis set by a few tens of percent going from cc-pVDZ to cc-pV5Z basis sets, the error that CCSD(T) makes does not grow in proportion.

Table I shows the difference between the SHCI total energies for the molecules and their constituent atoms, extrapolated to the CBS limit according to Eqs. (13) and (14). It also shows the ZPE, SR+SO, and CV corrections taken from the literature and the final prediction for the SHCI atomization energy D_0 and how much it differs from the best available experimental values. The difference between the SHCI D_0 and experiment is also plotted in Fig. 3, both before and after the corrections are applied.

There are 3 possible sources of discrepancy between the calculated and the experimental atomization energies: (1) The extrapolation to the CBS limit may not be accurate; (2) the literature values of the ZPE, SR+SO, and CV corrections may not be accurate; 3) the experimental values have errors. It seems likely, as discussed below, that all three of these play a role for some of the systems.

We show in Fig. 4 the convergence of the atomization energies with basis size. The SHCI atomization energies in fact have two extrapolation errors. The first and more benign error comes from extrapolating SHCI total energies for each basis set to the FCI limit, i.e., $\epsilon_1 \to 0$. This error can be reduced by employing smaller ϵ_1 and/or using better optimized orbitals. For the four basis sets n= 2 (D), 3 (T), 4 (Q), and 5, the largest extrapolation distances in the total energy of these 55 molecules and 12 atoms are 0.97, 2.36, 3.34, and 2.90 mHa, respectively.⁵⁵ Assuming that the extrapolated energies are in error by no more than a fifth of the extrapolation distance, all these energies should be accurate to considerably better than 1 mHa. Further, the typical extrapolation distances are much smaller, especially for the lighter systems: the median distances for the four basis sets are 2.92, 14.4, 56.4, and 77.0 μ Ha, respectively. The second source of error comes from extrapolation to the CBS limit, using Eqs. (13) and (14), and is less under control. For these 67 systems, the maximum and median CBS extrapolation distances are 29.4 and 6.48 mHa, respectively. This CBS extrapolation error is likely to be an important error for those systems where the extrapolation distance (the energy difference between the black dots and red crosses in Fig. 4) is large. The largest extrapolation distance by

TABLE I. Deviation of SHCI and SHCI+PBE atomization energies, D_0 , in the complete-basis-set limit from the best available experimental energies in units of kcal/mol. The raw SHCI and SHCI+PBE energies are corrected for zero-point energy (ZPE), scalar relativity (SR), spin-orbit energy (SO) and core-valence correlation (CV). For each molecule, the ZPE, SR+SO and CV corrections are taken from Ref. 50 if available, and otherwise from Ref. 24 as shown next to the ZPE correction. The only exceptions are that the CV corrections for LiH and Li₂ were taken from Ref. 24 because Ref. 50 did not freeze the core for these systems.

						SHCI		SHCI+PBE	
molecule	SHCI D_e	ZPE	SR+SO	CV	experiment	D_0	deviation	D_0	deviation
LiH	57.73	-1.99^{50}	-0.02	0.30	55.70^{53}	56.02	0.32	56.02	0.32
BeH	50.25	-2.92^{50}	-0.02	0.51	47.70^{54}	47.82	0.12	47.80	0.10
CH	84.12	-4.04^{50}	-0.08	0.14	79.97^{51}	80.14	0.17	80.16	0.19
$CH_2(^3B_1)$	190.04	-10.55^{50}	-0.23	0.82	179.83^{51}	180.08	0.25	179.95	0.12
$\operatorname{CH}_2(^1A_1)$	181.15	-10.29^{50}	-0.17	0.39	170.83^{51}	171.08	0.25	171.10	0.27
CH_3	306.98	-18.55^{50}	-0.25	1.07	289.11^{51}	289.25	0.14	289.18	0.07
CH_4	419.31	-27.74^{50}	-0.27	1.26	392.47^{51}	392.56	0.09	392.56	0.09
NH	83.11	-4.64^{50}	-0.07	0.11	78.36^{51}	78.51	0.15	78.55	0.19
NH_2	182.53	-11.84^{50}	0.08	0.32	170.59^{51}	171.09	0.50	171.10	0.51
NH_3	297.96	-21.33^{50}	-0.25	0.65	276.59^{51}	277.03	0.44	276.97	0.38
OH	107.28	-5.29^{50}	-0.24	0.14	101.73^{51}	101.89	0.16	101.81	0.08
$\rm H_2O$	233.05	-13.26^{50}	-0.49	0.38	219.37^{51}	219.68	0.31	219.51	0.14
HF	141.77	-5.86^{50}	-0.58	0.17	135.27^{51}	135.50	0.23	135.37	0.10
$\operatorname{SiH}_2(^1A_1)$	154.15	-7.30^{24}	-0.60	0.00	144.10^{53}	146.25	2.15	146.11	2.01
$SiH_2(^3B_1)$	133.47	-7.50^{24}	-0.80	-0.50	123.40^{24}	124.67	1.27	124.47	1.07
$SiH_2(B_1)$ SiH_3	228.54	-13.20^{24}	-0.80	-0.20	212.20^{53}	214.34	2.14	214.10	1.90
SiH_4	325.32	-19.40^{24}	-1.00	-0.20	302.60^{53}	304.72	2.12	304.41	1.81
PH_2	154.48	-8.40^{24}	-0.20	0.30	144.70^{24}	146.18	1.48	145.99	1.29
PH_3	242.38	-3.40 -14.44^{50}	-0.20	0.30	227.10^{53}	227.83	0.73	227.47	0.37
$_{\mathrm{H_2S}}^{\mathrm{H_3}}$	183.96	-9.40^{50}	-0.44	0.33 0.24	173.20^{53}	173.87	$0.73 \\ 0.67$	173.40	0.37
HCl		-9.40 -4.24^{24}	-0.93	0.24 0.30	173.20 102.21^{51}	102.59	0.07		0.20
	107.53	-4.24 -0.50^{50}			23.90^{53}			102.24	
Li_2	24.14	$-0.50^{\circ \circ}$ -1.30^{24}	0.00	0.20	137.60^{53}	23.84	-0.06	23.84	-0.06
LiF	138.15		-0.60	0.90		137.15	-0.45	137.34	-0.26
C_2H_2	403.19	-16.50^{50}	-0.46	2.47	388.64^{51}	388.70	0.06	388.84	0.20
C_2H_4	561.27	-31.66^{50}	-0.50	2.36	532.04^{51}	531.47	-0.57	531.58	-0.46
C_2H_6	711.47	-46.23^{50}	-0.56	2.42	666.19^{51}	667.10	0.91	666.97	0.78
CN	180.24	-2.95^{50}	-0.24	1.10	178.12^{51}	178.15	0.03	178.58	0.46
HCN	311.93	-9.95^{50}_{50}	-0.31	1.67	303.14^{51}	303.34	0.20	303.76	0.62
CO	258.61	-3.09^{50}	-0.46	0.95	256.23^{51}	256.01	-0.22	256.47	0.24
HCO	277.46	-8.09^{50}	-0.59	1.16	270.76^{51}	269.94	-0.82	270.28	-0.48
H_2CO	373.45	-16.52^{50}	-0.65	1.30	357.48^{51}	357.58	0.10	357.88	0.40
H_3COH	512.51	-31.72^{24}	-0.80	1.50	480.97^{51}	481.49	0.52	481.52	0.55
N_2	227.66	-3.36^{50}	-0.14	0.80	224.94^{51}	224.96	0.02	225.62	0.68
N_2H_4	438.68	-32.68^{50}	-0.51	1.14	404.81^{51}	406.63	1.82	406.60	1.79
NO	152.33	-2.71^{50}	-0.23	0.42	149.81^{51}	149.81	0.00	150.23	0.42
O_2	120.50	-2.25^{50}	-0.62	0.24	117.99^{51}	117.87	-0.12	117.95	-0.04
$\mathrm{H_2O_2}$	269.25	-16.44^{50}	-0.82	0.36	252.21^{51}	252.35	0.14	252.33	0.12
F_2	39.09	-1.30^{50}	-0.79	-0.11	36.93^{51}	36.89	-0.04	36.93	0.00
CO_2	388.19	-7.24^{50}	-1.01	1.77	381.98^{51}	381.71	-0.27	382.46	0.48
Na_2	16.65	-0.20^{24}	0.00	0.30	17.00^{53}	16.75	-0.25	16.78	-0.22
Si_2	74.64	-0.73^{50}	-1.01	0.13	74.40^{53}	73.03	-1.37	72.68	-1.72
P_2	116.99	-1.11^{50}	-0.25	0.77	116.00^{53}	116.40	0.40	116.40	0.40
S_2	104.55	-1.04^{50}	-1.40	0.34	100.80^{53}	102.45	1.65	101.62	0.82
Cl_2	60.27	-0.80^{50}	-1.82	-0.13	57.18^{51}	57.52	0.34	56.70	-0.48
NaCl	99.73	-0.50^{24}	-1.10	-1.20	97.40^{53}	96.93	-0.47	96.56	-0.84
SiO	192.46	-1.78^{50}	-0.90	0.95	189.80^{53}	190.73	0.93	190.80	1.00
CS	171.88	-1.83^{50}	-0.80	0.75	170.40^{53}	170.00	-0.40	169.72	-0.68
SO	126.97	-1.63^{50}	-1.09	0.41	123.50^{53}	124.66	1.16	123.99	0.49
ClO	65.99	-1.22^{50}	-0.81	0.06	63.42^{51}	64.02	0.60	63.18	-0.24
ClF	63.26	-1.22 -1.12^{50}	-0.31	-0.10	60.35^{51}	60.65	0.30	60.07	-0.24
Si_2H_6	536.27	-30.50^{24}	-2.00	0.00	500.10^{24}	503.77	3.67	503.39	3.29
	395.23	-30.50 -23.19^{24}		1.20	371.35^{51}	371.84			0.15
CH ₃ Cl		-23.19^{-2} -28.60^{24}	-1.40				0.49	371.50	
H ₃ CSH	474.86	-28.60^{24} -8.18^{24}	-1.20	1.50	445.10^{53}	446.56	1.46	445.98	0.88
HOCl	166.90		-1.50	0.40	156.88^{51}	157.62	0.74	156.99	0.11
SO_2	264.04	-4.38^{50}	-1.79	0.92	254.46^{52}	258.79	4.33	257.00	2.54

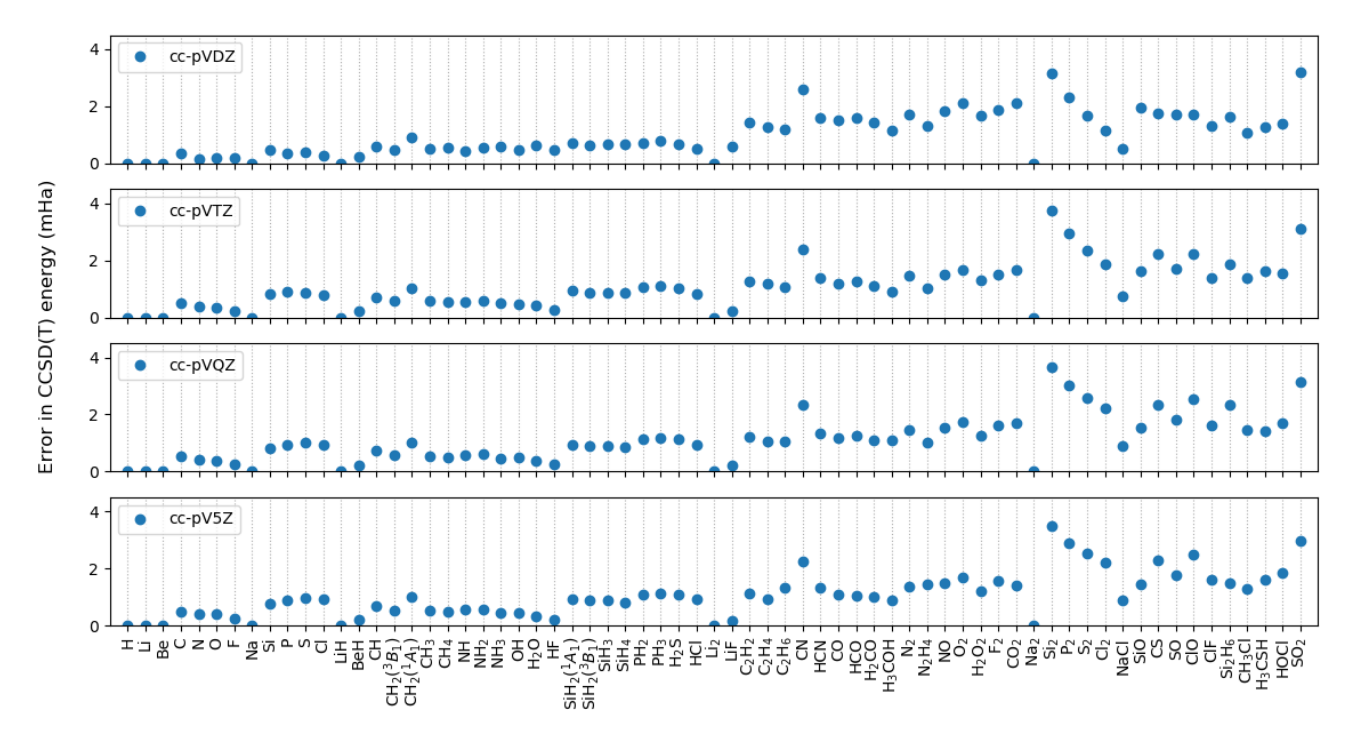


FIG. 2. The error in the CCSD(T) total energies obtained by comparison to the SHCI total energies. The CCSD(T) errors are of course zero for systems with one or two valence electrons, and they are positive in all other cases. The errors for each system are very similar for the various basis sets, especially for the larger basis sets.

far is for SO_2 , the molecule for which we have the largest deviation from experiment. It has been argued in the literature that larger basis sets are needed for SO_2 in order to obtain an accurate CBS extrapolation⁵⁶.

To explore further the issue of the CBS extrapolation error, we add the PBE-based basis-set correction to the SHCI energies for each basis set [see Eqs. (15) and (16)] and also extrapolate the corrected energies to the CBS limit according to Eq. (21), which gives us an alternative way to estimate the CBS limit of the SHCI energies. The PBE-based corrections can also be found in the Supplemental Materials⁴⁹. It is apparent from Table I that the deviations of the SHCI and the SHCI+PBE energies from experiment are strongly correlated, thereby giving us a reasonable measure of confidence in our two extrapolations as well as an estimate of the extrapolation errors. Fig. 5 shows the same information as Fig. 4 after the PBE-based basis-set correction has been included. As summarized in Table II, for each basis set the MAD from experiment decreases by about a factor of 3 compared to that without the basis-set correction.⁵⁷ In particular, SHCI+PBE gives a MAD below 1 kcal/mol already with the cc-pVQZ basis set. The cc-pV5Z basis set has a MAD of only 0.52 kcal/mol. Applying the CBS extrapolation to SHCI+PBE gives a somewhat larger MAD from experiment of 0.61 kcal/mol, as the computed atomization energies are too small for the smaller basis sets but increase with increasing basis size and for the majority of the molecules the computed CBS atomization energies

are larger than experiment.

As seen from Figs. 4 and 5 the predicted CBS atomization energy of $\mathrm{Si_2H_6}$ is more than 3 kcal/mol larger than experiment. However, unlike $\mathrm{SO_2}$, even the ccpV5Z value is larger than experiment, so the discrepancy cannot be attributed to an inaccurate CBS extrapolation, but instead to either inaccurate ZPE, SR+SO, and CV correction, or, to errors in the experimental value. In fact, the same holds for all six molecules in Fig. 5 that have cc-pV5Z atomization energies that are larger than experiment by more than 1 kcal/mol. Note that the number of systems for which the atomization energies are overestimated in Figs. 4 and 5 is greater than the number of systems for which they are underestimated.

The majority of the deviations fall below 1 kcal/mol, reaching chemical accuracy as can be seen in Table I and Figs. 4 and 5. As regards those where the deviations are larger than 1 kcal/mol it should also be kept in mind that the experimental values may be inaccurate, particularly for those atomization energies that are not available from the ATcT database⁵¹. For example, for PH₂ the two available experimental values differ by 4.5 kcal/mol and our computed value differs by +1.5 kcal/mol from Ref. 24 and -3.0 kcal/mol from Ref. 53. For the molecules in the ATcT database the MAD is only 0.35 kcal/mol before the PBE-based correction is applied and 0.34 kcal/mol after it is applied.

Compared to other methods, our MAD of 0.61 kcal/mol is significantly less than the MAD of 1.2 to 3.2

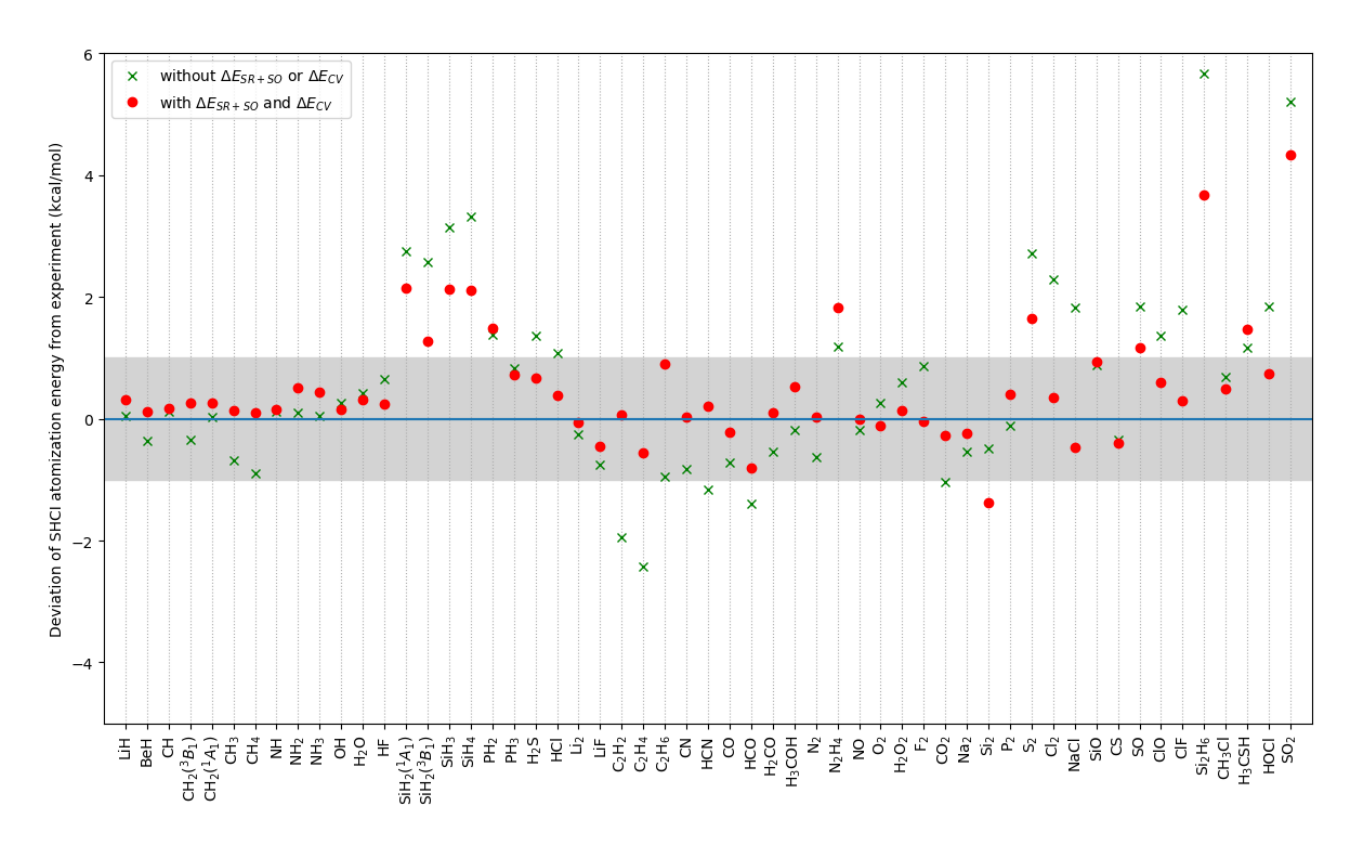


FIG. 3. The comparison of SHCI atomization energies in the extrapolated complete-basis-set limit with experiment, with (red dots) and without (green crosses) scalar relativistic and spin-orbit (SR+SO) corrections and core-valence (CV) corrections. Both sets of points include zero-point energy (ZPE) corrections. Systems for which red dots fall in the shaded region are considered to have reached chemical accuracy (1 kcal/mol).

TABLE II. Summary statistics of deviations from experimental atomization energies for the 55 molecules. For each of the basis sets the inclusion of the PBE-based basis-set correction reduces the MAD by about a factor of 3. MAD: mean absolute deviation. MAX: maximum absolute deviation. Units: kcal/mol.

AX .65
.09
.54
.20
.33
.05
.68
.76
.06
.29
, i

kcal/mol obtained in various QMC studies^{28–30}. Diffusion Monte Carlo works directly in the CBS limit, but the fixed-node approximation is the dominant error. Using trial wave functions with Slater determinants chosen from a SCI method, it should be easily possible

to reduce considerably the fixed-node error as demonstrated in Refs. 15, 58, and 59. Our MAD is comparable to results reported from composite coupled-cluster-based methods^{24,60,61}. The HEAT studies performed all-electron calculations using the coupled-cluster method with up to quadruple excitations on a somewhat different set of molecules consisting solely of first-row elements²⁵. For the 19 molecules also present in the G2 set, the MAD of HEAT, SHCI, and SHCI+PBE are 0.07, 0.21, and 0.28 kcal/mol, respectively. It should be noted that HEAT is a composite quantum chemistry method, and for the lower levels of theory it employs larger basis sets than those we used, thereby significantly reducing the CBS extrapolation error.

VII. CONCLUSION AND OUTLOOK

The SHCI method enables the calculation of essentially exact energies within basis sets up to cc-pV5Z of all the molecules in the G2 set. After extrapolation to the CBS limit and addition of ZPE, SR+SO and CV corrections, the MAD from the experimental atomization energies is only $0.61~\rm kcal/mol$. However, there are 8 molecules where

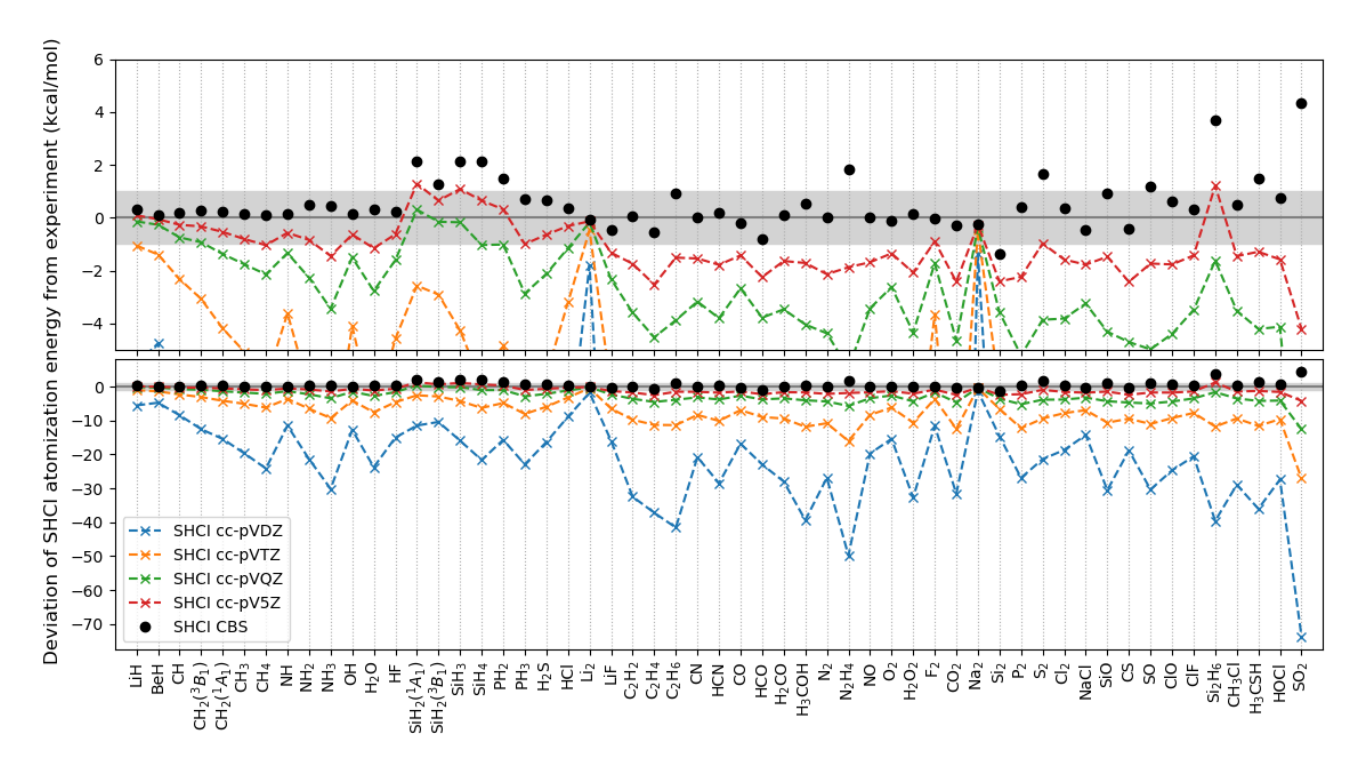


FIG. 4. The comparison of SHCI atomization energies with experiment in the individual basis sets and in the extrapolated complete-basis-set limit. The top panel is a blowup of the top portion of the bottom panel. The shaded region indicates chemical accuracy (1 kcal/mol).

the computed atomization energy is more than 1 kcal/mol larger than experiment and 1 molecule for which it is more than 1 kcal/mol smaller than experiment. These differences are probably due to a combination of errors in the computations and experiments. With additional computational effort it would be possible to reduce the uncertainties in the computed energies. First, instead of adding on a CV energy correction, one could use the cc-pwCVnZ basis sets to include the correlation contribution from the core electrons. This could also make the basis-set extrapolation more reliable. Although this entails a large increase in the Hilbert space, the increase in the computational cost of the SHCI is not prohibitive because relatively few of the core excitations have a large amplitude. Second, relativistic effects could also be included within the SHCI method, as has already been demonstrated⁶². Third, the computation of the ZPE correction would require calculating derivatives with respect to the nuclear coordinates. This could also be done, but would probably be the most computationally expensive part of the calculation. Fourth, the CBS extrapolation could be improved either by employing better basis sets or using a better DFT-based basis-set correction. With these improvements, the computed energies could have the potential to be sufficiently accurate to reliably pinpoint errors in experimental values of atomization energies.

ACKNOWLEDGMENTS

This work was supported in part by the AFOSR under grant FA9550-18-1-0095. Y.Y. acknowledges support from the Molecular Sciences Software Institute, funded by U.S. National Science Foundation grant ACI-1547580. Some of the computations were performed at the Bridges cluster at the Pittsburgh Supercomputing Center supported by NSF grant ACI-1445606. We thank Pierre-François Loos for valuable comments on the manuscript.

DATA AVAILABILITY

The data that support the findings of this study are available within the article and the supplementary material of the arXiv version of this paper⁶³.

¹A. A. Holmes, N. M. Tubman, and C. J. Umrigar, J. Chem. Theory Comput. **12**, 3674 (2016).

²S. Sharma, A. A. Holmes, G. Jeanmairet, A. Alavi, and C. J. Umrigar, J. Chem. Theory Comput. 13, 1595 (2017).

³A. A. Holmes, C. J. Umrigar, and S. Sharma, J. Chem. Phys. 147, 164111 (2017).

⁴J. E. Smith, B. Mussard, A. A. Holmes, and S. Sharma, J. Chem. Theory Comput. **13**, 5468 (2017).

⁵B. Mussard and S. Sharma, J. Chem. Theory Comput. **14**, 154 (2017)

⁶A. D. Chien, A. A. Holmes, M. Otten, C. J. Umrigar, S. Sharma, and P. M. Zimmerman, J. Phys. Chem. A **122**, 2714 (2018).

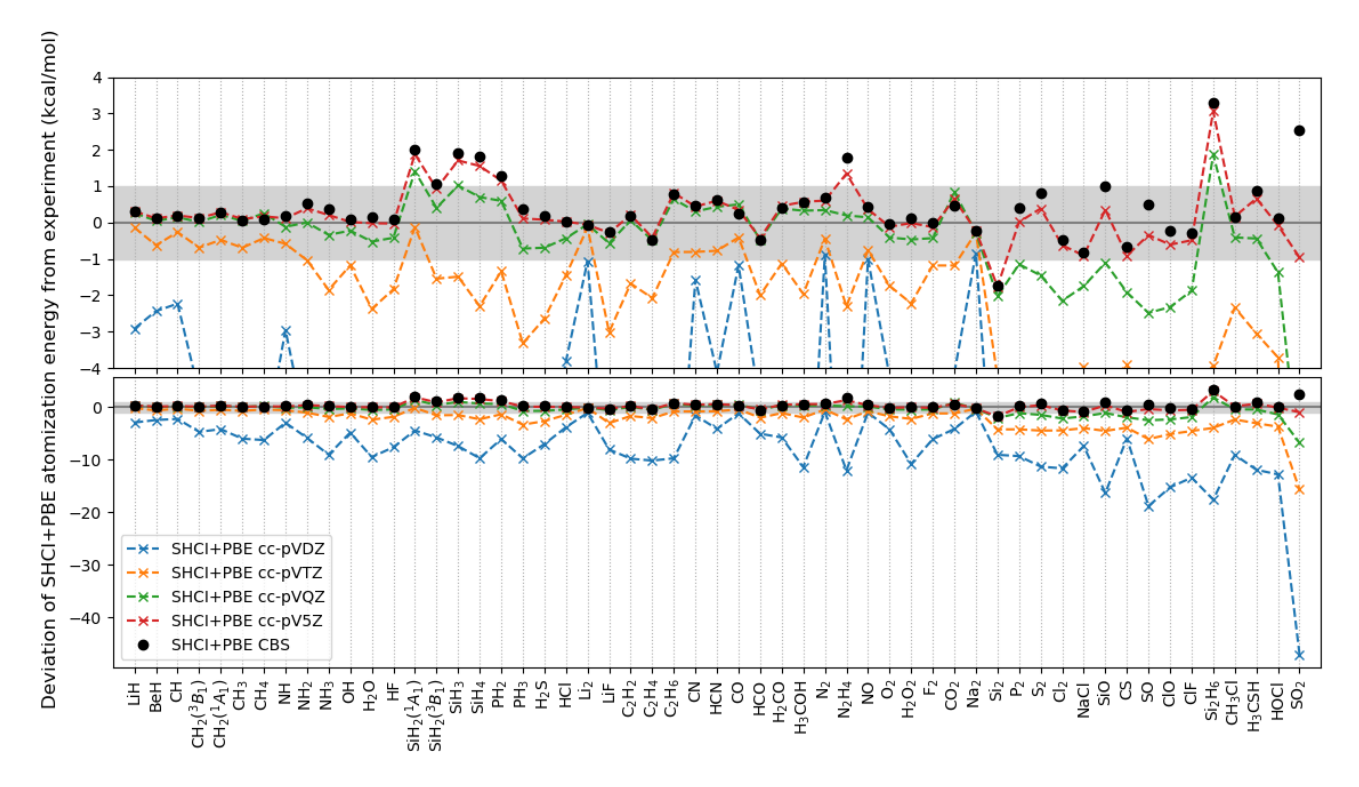


FIG. 5. Same as Fig. 4 but with the PBE-based basis set correction applied.

- ⁷J. Li, M. Otten, A. A. Holmes, S. Sharma, and C. J. Umrigar, J. Chem. Phys. **149**, 214110 (2018).
- ⁸J. Li, Y. Yao, A. Holmes, M. Otten, S. Sharma, and C. J. Umrigar, Phys. Rev. Research **2**, 012015(R) (2020).
- ⁹K. T. Williams, Y. Yao, J. Li, L. Chen, H. Shi, M. Motta, C. Niu, U. Ray, S. Guo, R. J. Anderson, J. Li, L. N. Tran, C.-N. Yeh, B. Mussard, S. Sharma, F. Bruneval, M. van Schilfgaarde, G. H. Booth, G. K.-L. Chan, S. Zhang, E. Gull, D. Zgid, A. Millis, C. J. Umrigar, and L. K. Wagner, Phys. Rev. X 10, 011041 (2020).
- ¹⁰C. F. Bender and E. R. Davidson, Phys. Rev. **183**, 23 (1969).
- ¹¹J. Whitten and M. Hackmeyer, J. Chem. Phys **51**, 5584 (1969).
- ¹²B. Huron, J. P. Malrieu, and P. Rancurel, J. Chem. Phys. 58, 5745 (1973).
- ¹³R. J. Buenker and S. D. Peyerimhoff, Theor. Chim. Acta 35, 33 (1974).
- ¹⁴S. Evangelisti, J.-P. Daudey, and J.-P. Malrieu, Chem. Phys. **75**, 91 (1983).
- ¹⁵E. Giner, A. Scemama, and M. Caffarel, Can. J. Chem. **91**, 879 (2013).
- ¹⁶F. A. Evangelista, J. Chem. Phys. **140**, 124114 (2014).
- ¹⁷A. Scemama, T. Applencourt, E. Giner, and M. Caffarel, J. Comp. Chem. 37, 1866 (2016).
- ¹⁸Y. Garniron, A. Scemama, P.-F. Loos, and M. Caffarel, J. Chem. Phys. **147**, 034101 (2017).
- ¹⁹P.-F. Loos, A. Scemama, A. Blondel, Y. Garniron, M. Caffarel, and D. Jacquemin, J. Chem. Theory Comput. **14**, 43604379 (2018).
- ²⁰D. Hait, N. M. Tubman, D. S. Levine, K. B. Whaley, and M. Head-Gordon, J. Chem. Theory Comput. 15, 5370 (2019).
- ²¹P.-F. Loos, F. Lipparini, M. Boggio-Pasqua, A. Scemama, and D. Jacquemin, J. Chem. Theory Comput. 16, 1711 (2020).
- ²²L. A. Curtiss, K. Raghavachari, G. W. Trucks, and J. A. Pople, J. Chem. Phys. **94**, 7221 (1991).
- ²³L. A. Curtiss, P. C. Redfern, and K. Raghavachari, J. Chem. Phys. **126**, 084108 (2007).
- ²⁴D. Feller and K. A. Peterson, J. Chem. Phys. **110**, 8384 (1999).

- ²⁵ A. Tajti, P. Szálay, A. Csaszar, M. Kállay, J. Gauss, E. Valeev, B. Flowers, J. Vázquez, and J. Stanton, J. Chem. Phys. **121**, 11599 (2004).
- ²⁶A. Karton, E. Rabinovich, J. M. L. Martin, and B. Ruscic, J. Chem. Phys. **125**, 144108 (2006).
- ²⁷J. H. Thorpe, C. A. Lopez, T. L. Nguyen, J. H. Baraban, D. H. Bross, B. Ruscic, and J. F. Stanton, J. Chem. Phys. **150**, 224102 (2019).
- ²⁸ Jeffrey C. Grossman, Phys. Rev. Lett. **117**, 1434 (2002).
- ²⁹N. Nemec, M. D. Towler, and R. J. Needs, J. Chem. Phys. **132**, 034111 (2010).
- ³⁰F. R. Petruzielo, J. Toulouse, and C. J. Umrigar, J. Chem. Phys. 136, 124116 (2012).
- ³¹M. Caffarel, T. Applecourt, E. Giner, and A. Scemama, in Recent Progress in Quantum Monte Carlo, ACS Symposium Series, Vol. 1234 (2016) pp. 15–46.
- ³²E. Giner, B. Pradines, A. Ferté, R. Assaraf, A. Savin, and J. Toulouse, J. Chem. Phys. **149**, 194301 (2018).
- ³³P.-F. Loos, B. Pradines, A. Scemama, J. Toulouse, and E. Giner, J. Phys. Chem. Lett. **10**, 2931 (2019).
- ³⁴E. Giner, A. Scemama, J. Toulouse, and P.-F. Loos, J. Chem. Phys. **151**, 144118 (2019).
- ³⁵E. Giner, A. Scemama, P.-F. Loos, and J. Toulouse, J. Chem. Phys. **152**, 174104 (2020).
- ³⁶Since the absolute values of c_i for the most important determinants tends to go down as more determinants are included in the wave function, a somewhat better selection of determinants is obtained by using a larger value of ϵ_1 in the initial iterations.
- ³⁷E. R. Davidson, Comput. Phys. Commun. **53**, 49 (1989).
- ³⁸P. S. Epstein, Phys. Rev. **28**, 695 (1926).
- ³⁹R. K. Nesbet, Proc. R. Soc. London, Ser. A. **230**, 312 (1955).
- ⁴⁰S. J. Reddi, S. Kale, and S. Kumar, ICLR Published as a conference paper at the International Conference on Learning Representations, 2018.
- ⁴¹T. Helgaker, W. Klopper, H. Koch, and J. Noga, J. Chem. Phys. 106, 9639 (1997).

- ⁴²A. Halkier, T. Helgaker, P. Jørgensen, W. Klopper, H. Koch, J. Olsen, and A. K. Wilson, Chem. Phys. Lett. **286**, 243 (1998).
- ⁴³A. Halkier, T. Helgaker, P. Jørgensen, W. Klopper, and J. Olsen, Chem. Phys. Lett. **302**, 437 (1999).
- ⁴⁴J. P. Perdew, K. Burke, and M. Ernzerhof, Phys. Rev. Lett. **77**, 3865 (1996).
- ⁴⁵O. Franck, B. Mussard, E. Luppi, and J. Toulouse, J. Chem. Phys. **142**, 074107 (2015).
- ⁴⁶Q. Sun, T. C. Berkelbach, N. S. Blunt, G. H. Booth, S. Guo, Z. Li, J. Liu, J. McClain, S. Sharma, S. Wouters, and G. K.-L. Chan, WIREs Comput. Mol. Sci. 8, e1340 (2018).
- ⁴⁷H.-J. Werner, P. J. Knowles, G. Knizia, F. R. Manby, and M. Schütz, Wiley Interdiscip. Rev.: Comput. Mol. Sci. 2, 242 (2012).
- ⁴⁸Y. Garniron, T. Applencourt, K. Gasperich, A. Benali, A. Ferté, J. Paquier, B. Pradines, R. Assaraf, P. Reinhardt, J. Toulouse, P. Barbaresco, N. Renon, G. David, J.-P. Malrieu, M. Véril, M. Caffarel, P.-F. Loos, E. Giner, and A. Scemama, J. Chem. Theory Comput. 15, 3591 (2019).
- ⁴⁹Supplemental materials.
- ⁵⁰D. Feller, K. A. Peterson, and D. A. Dixon, J. Chem. Phys. **129**, 204105 (2008).
- ⁵¹B. Ruscic and D. H. Bross, Active Thermochemical Tables (ATcT) values based on ver. 1.122g of the Thermochemical Network (2019), see https://atct.anl.gov/.
- ⁵²B. Ruscic, A. Fernandez, J. M. L. Martin, R. E. Pinzon, D. Kodeboyina, G. von Laszewski, D. G. Archer, R. D. Chirico, M. Frenkel, and J. W. Magee, unpublished results obtained from Active Thermochemical Tables ver. 1.25 using the adjunct Thermochemical Network describing key sulfur-containing species ver.

- 1.056a, as reported in Ref. 26.
- ⁵³ "NIST computational chemistry comparison and benchmark database," Release 20, August 2019, Editor: Russell D. Johnson III.
- ⁵⁴M. Vasiliu, K. A. Peterson, and D. A. Dixon, J. Chem. Theory Comput. **13**, 649 (2017).
- ⁵⁵The extrapolation distance depends on the value of ϵ_1 in Eq. 2 and on how well the orbitals are optimized to improve the convergence of the energy.
- ⁵⁶C. W. Bauschlicher Jr. and A. Ricca, J. Phys. Chem. A **102**, 8044 (1998).
- 57To avoid confusion, we note that in Ref. 33 it was found that CCSD(T)+PBE had a MAD of only 1.96, 0.85, and 0.31 kcal/mol with respect to the CCSD(T) CBS limit for the cc-pVDZ, cc-pVTZ, and cc-pVQZ basis sets, respectively. These considerably smaller values compared to those in Table II are the result of a one-body basis-set correction that was always included by adding the cc-pV5Z HF energy to the CCSD(T) correlation energies for the different basis sets. Of course one could do the same for the SHCI energies in the current paper.
- ⁵⁸E. Giner, R. Assaraf, and J. Toulouse, Mol. Phys. **114**, 910 (2016).
- ⁵⁹M. Dash, S. Moroni, A. Scemama, and C. Filippi, J. Chem. Theory Comput. 14, 4176 (2018).
- ⁶⁰J. Martin and G. de Oliveira, J. Chem. Phys. **111**, 1843 (1999).
- ⁶¹R. Haunschild and W. Klopper, J. Chem. Phys. **136**, 164102 (2012).
- ⁶²B. Mussard and S. Sharma, J. Chem. Theory Comput. **14** (2018), DOI: 10.1021/acs.jctc.7b01019.
- ⁶³Y. Yao, E. Giner, J. Li, J. Toulouse, and C. J. Umrigar, https://arxiv.org/abs/2004.10059.